Journal of Thermal Analysis and Calorimetry, Vol. 61 (2000) 827–837

STUDIES ON THE STATE OF Fe AND La IN MCM-41 MESOPOROUS MOLECULAR SIEVE MATERIALS BY TG ANALYSIS AND OTHER TECHNIQUES

N. He[1,2,3], *C. Yang*[4], *Q. Dai*[1], *J. Wang*[5], *C. Yuan*[1] *and Z. Lu*[1,3]

[1]National Laboratory of Molecular and Biomolecular Electronics, Southeast University Nanjing 210096
[2]Department of Chemistry, Xiangtan University, Xiangtan 411105
[3]Nanjing E-life Gene Company Ltd., Nanjing 210016
[4]Nanjing Normal University, Nanjing 210024
[5]Nanjing Analytical Instrument Factory, Nanjing 210017, P. R. China

(Received January 23, 1999; in revised form December 10, 1999)

Abstract

Siliceous MCM-41 mesoporous materials and those possessing Fe, La, Al, respectively, were synthesized using water glass as silica source. Results from thermogravimetric analysis and other techniques showed us that Fe(III) or La(III) species was incorporated into framework. Owing to Fe–O or La–O bond longer than Si–O bond, Fe(III) or La(III) species was limited to insert into framework and transformed from tetrahedrally coordinated state to octahedrally coordinated state upon calcination to remove template.

Keywords: iron, lanthanum, MCM-41 mesoporous materials, states, thermogravimetric analysis

Introduction

Since the average pore size is usually smaller than 0.7 nm, the application of microporous zeolite molecular sieve materials was limited when used as a sorbent or a catalytic material for large organic and inorganic compounds. Therefore, the synthesis of a hexagonal mesoporous molecular sieve family (designated as MCM-41) by researchers at the Mobil Company in 1992 [1, 2] was a breakthrough of zeolite molecular sieve research and material science. The average pore size of this kind of new material can be adjusted between 1.8–10 nm, leading us to new materials for use as sorbents, catalyst materials, host materials for host-guest chemistry in studies of electron transfer photosensitizers [3], semiconductors [4], polymer wires [5–8], conducting carbon wires [9], sensing devices [10], materials with non-linear optic properties [11], quantum sized clusters [11, 12], etc.

Fe-containing or La-containing molecular sieve materials are two very important kinds of catalysts [13]. Siliceous, aluminum silicate, and Fe- or La-containing

1418–2874/2000/ $ 5.00
Akadémiai Kiadó, Budapest

MCM-41 mesoporous materials can be easily synthesized using water glass as silicon source [14]. The synthesis and the investigation of the thermal and hydrothermal stability of those materials has been reported in detail in our previous report [14], but the states of Fe or La species were not characterized in detail. The further evidence of the incorporation of Fe, La into the framework (channel wall) of these samples was presented here by thermogravimetric analysis (TG), framework vibration Fourier transform infrared (FT-IR) spectroscopic method, powder X-ray diffraction (XRD), electron spin resonance (ESR) and Mössbauer spectroscopic techniques.

Experimental

FeSiMCM-41 mesoporous materials with different Fe content were prepared according to the following synthesis procedures: 11 g distilled water, 0.4 g sulphuric acid (95%) and optionally, different amounts of $Fe(NO_3)\cdot 9\,H_2O$, varying from 0 to 0.71 g, were mixed and stirred for 10 min. Then 8.6 g water glass (20.3% SiO_2, 6.7% Na_2O) were added. After stirring the formed mixture for 10 min, the appropriate amount template solution (25% $C_{16}H_{33}(CH_3)_3NBr$, CTABr) was added. The formed gel was stirred for 30 min before adding 6.7 g distilled water. Then the gel was transferred into a stopped teflon-lined steel bottle and heated without stirring at 373 K for 7 days. After cooled to room temperature, the resulting solid product was recovered by filtration, extensively washed with distilled water, and dried in air at ambient temperature. The preparation of LaSiMCM-41 mesoporous materials was similar to that mentioned above except for substituting lanthanum nitrate for ferric nitrate. For comparison, AlSiMCM-41 sample was also synthesized by means of adding a given amount of sodium aluminate into the gel mixture instead of ferric nitrate.

The thermogravimetric analysis of samples in synthesized or calcined form were conducted on a thermoflex analyzer (Rigaku) in air up to 1073 K using a heating rate of 20 K min^{-1} and about 10 mg samples. The low-angle powder X-ray diffraction patterns were recorded on a Rigaku (D/max-γ A) X-ray diffraction instrument with Cu-K_α radiation. Framework vibration Fourier transform infrared spectra were recorded on a Nicolet 510 P FTIR spectrometer using the KBr pellet technique. Electron spin resonance spectra were investigated on a Bruker EP 200-D-SCR instrument. The Mössbauer spectra investigation were performed on a constant acceleration Mössbauer spectrometer with a source of ^{57}Co in Pd matrix. The adsorption of nitrogen at 77 K was conducted on a Micromeritics ASAP2000 instrument. The compositions of samples were obtained on a Jarrell-Ash 1100 inductively coupled plasma quantometer.

Results and discussion

The Si/Me (*M*=Fe, La) bulk ratios by chemical analysis for the as-synthesized samples are given in Table 1. The powder XRD patterns of these as-synthesized samples (Figs 1–3) and their calcined forms (Fig. 4) show two to four peaks in the region 1–8°2θ indexed on a hexagonal lattice typical of MCM-41 materials [1–2]. It seems

Table 1 Composition of gel mixtures and as-synthesized samples

Samples	Molar composition of the gel mixtures							As-synthesized samples		
	CTAB	SiO_2	Al_2O_3	Fe_2O_3	La_2O_3	Na_2O	H_2O	SiO_2/Al_2O_3	SiO_2/Fe_2O_3	SiO_2/La_2O_3
SiMCM-41	0.25	1.0	–	–	–	0.2	57.0	–	–	–
AlSiMCM-41(118)	0.25	1.0	0.008	–	–	0.2	57.0	118	–	–
AlSiMCM-41(58)	0.25	1.0	0.015	–	–	0.2	57.0	58	–	–
AlSiMCM-41(32)	0.25	1.0	0.030	–	–	0.2	57.0	32	–	–
FeSiMCM-41(124)	0.25	1.0	–	0.008	–	0.2	57.0	–	124	–
FeSiMCM-41(62)	0.25	–	–	0.015	–	0.2	57.0	–	62	–
FeSiMCM-41(32)	0.25	–	–	0.030	–	0.2	57.0	–	32	–
LaSiMCM-41(147)	0.25	–	–	–	0.008	0.2	57.0	–	–	147
LaSiMCM-41(83)	0.25	–	–	–	0.015	0.2	57.0	–	–	83
LaSiMCM-41(48)	0.25	–	–	–	0.030	0.2	57.0	–	–	48

that incorporation of Fe(III) or La(III) does not change the hexagonal structural form. It would be helpful to us to understand the states of Fe(III) and La(III) species in these samples.

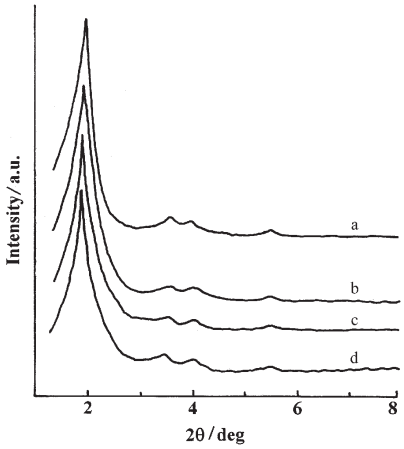

Fig. 1 XRD patterns for as-synthesized a – SiMCM-41; b – AlSiMCM-41(118); c – AlSiMCM-41(58); d – AlSiMCM-41(32)

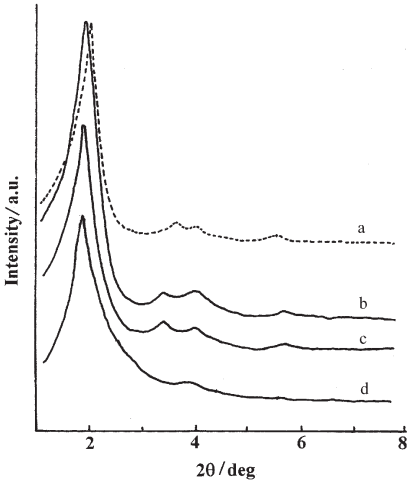

Fig. 2 XRD patterns for as-synthesized a – SiMCM-41; b – FeSiMCM-41(124); c – FeSiMCM-41(62); d – FeSiMCM-41(32)

As reported in literature [2, 15], templates associated with different inorganic components of MCM-41-type mesoporous materials will decompose and be removed at different temperature. Thus thermogravimetric analysis is one of the powerful tools to investigate the state of inorganic components in MCM-41 samples. The thermogravimetric curves of all the above as-synthesized samples are shown in Figs 5–7. Two steps can be

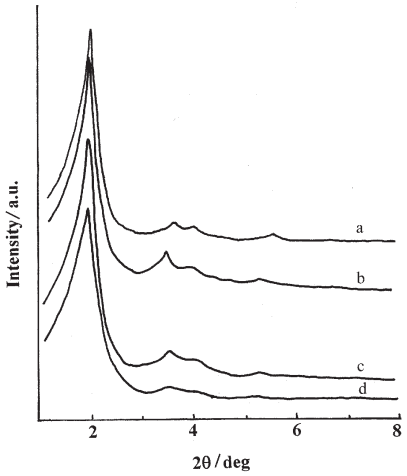

Fig. 3 XRD patterns for as-synthesized for a – SiMCM-41; b – LaSiMCM-41(147); c – LaSiMCM-41(83); d – LaSiMCM-41(48)

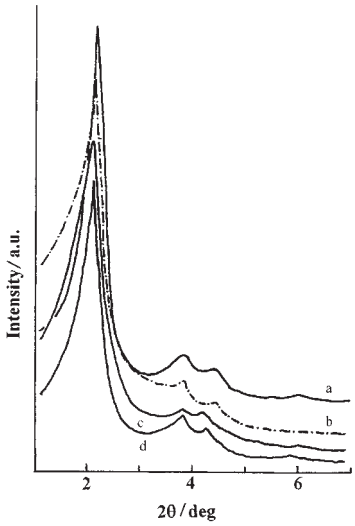

Fig. 4 XRD patterns for calcined a – SiMCM-41, b – AlSiMCM-41(58); c – FeSiMCM-41(62); d – AlSiMCM-41(83)

clearly observed in the TG curves of as-synthesized SiMCM-41 and AlSiMCM-41. The low-temperature step (450–620 K) was attributed to the decomposition of template interacting with siloxy group sites, while the step in high-temperature range was attributed to the decomposition of template associated with aluminum species in channel wall (framework) [2, 15]. The aluminum species in SiMCM-41 should come from the silica source, water glass, as impurity. The high-temperature step for SiMCM-41 is, therefore, much shorter than that for AlSiMCM-41.

Figures 6 and 7 clearly show us that as a result of introduction of Fe(III) or La(III) into MCM-41, a new step (600–710 K for LaSiMCM-41, 530–620 K for FeSiMCM-41, respectively) appears in the TG curves for the as-synthesized LaSiMCM-41 and FeSiMCM-41, respectively, strongly supporting the incorporation of Fe(III) or La(III) into the channel wall of these mesoporous materials. Moreover, the step associated with La(III) species exhibits a higher temperature range than the step associated with Fe(III) species indicates a stronger interaction between template and La(III) species than that between template and Fe(III) species. This TG analysis result is in consistence with the one from XRD characterization.

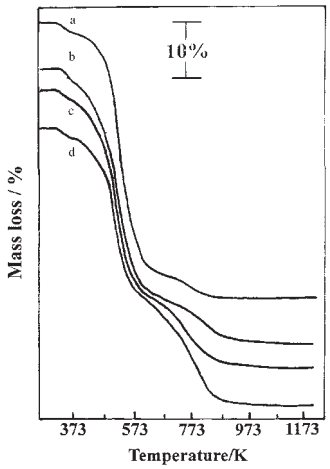

Fig. 5 Thermogravimetric analysis of as-synthesized samples. a – SiMCM-41; b – AlSiMCM-41(118); c – AlSiMCM-41(58); d – AlSiMCM-41(32)

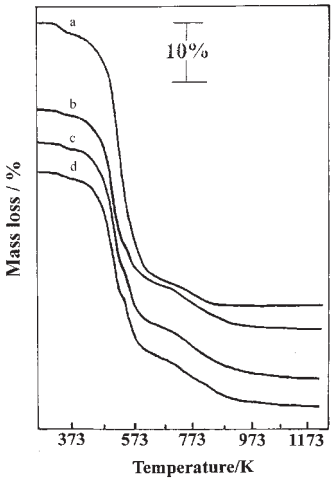

Fig. 6 Thermogravimetric analysis of as-synthesized samples. a – SiMCM-41; b – FeSiMCM-41(124); c – FeSiMCM-41(62); d – FeSiMCM-41(32)

It is evident from Fig. 2 that compared with the XRD peaks for as-synthesized SiMCM-41, the XRD peaks for as-synthesized FeSiMCM-41 and LaSiMCM-41 shift to low 2θ, indicating some Si–O bonds (0.161 nm) have been replaced by longer Fe–O (0.197 nm) or La–O (0.254 nm) bonds [16–17]. Although no effective characterization techniques but XRD and FT-IR are reported to characterize the states of La(III) species in zeolites, the structural arrangement of iron species in zeolite molecular sieve materials is also easily detectable by other methods such as ESR [18–19] and Mössbauer spectra [13] of Fe-containing zeolite molecular sieve samples. As depicted in Fig. 8, two different signals occur in the spectra of the as-synthesized FeSiMCM-41 samples. The signal with g=4.3 was assigned to Fe(III) in distorted framework tetrahedral coordination whereas the signal with g=2.0 belongs to Fe(III) in a highly symmetric octahedrally coordinated environment [18–19]. Taking it into consideration that the signal of g=2.0 is much more sensitive to the content of Fe(III)

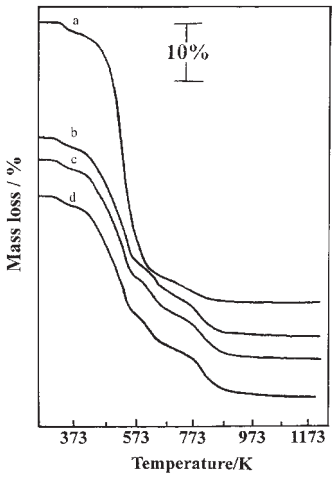

Fig. 7 Thermogravimetric analysis of as-synthesized samples. a – SiMCM-41; b – LaSiMCM-41(147); c – LaSiMCM-41(83); d – LaSiMCM-41(48)

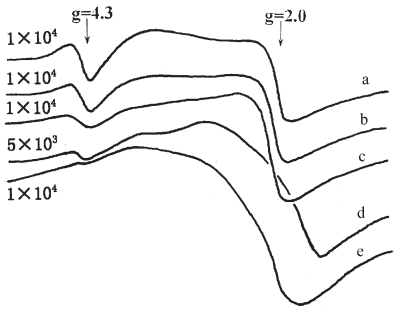

Fig. 8 ESR spectra for as-synthesized a – FeSiMCM-41(124); b – FeSiMCM-41(62); c – FeSiMCM-41(32) and d – calcined FeSiMCM-41(62) at 813 K in air for 1 h; e – calcined FeSiMCM-41(62) at 813 K in air for 4 h

species in an octahedrally coordinated environment, Fig. 8 shows us that the introduced Fe(III) species mainly locate in framework positions. It is well known that Mössbauer spectroscopy is another very useful tool to study the state of Fe species in zeolite molecular sieve materials. If in tetrahedrally coordinated state, Fe(III) species will give an isomer shift (IS) value smaller than 0.3 mm s^{-1} in contrast to the IS value greater than 0.3 mm s^{-1} typical of octahedrally coordinated Fe(III) species [13].

Figure 9 shows the Mössbauer spectrum for FeSiMCM-41(64) (Fig. 9a), the IS value for this sample is 0.28, correspondent with tetrahedrally coordinated Fe(III) in

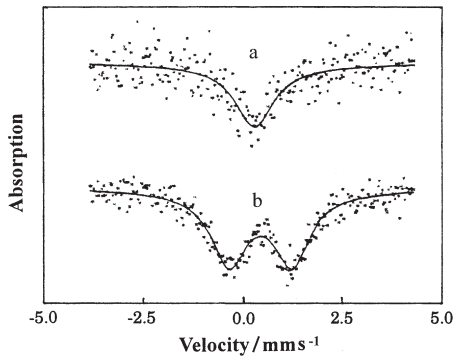

Fig. 9 Mössbauer spectra for a – as-synthesized FeSiMCM-41(62) and b – calcined FeSiMCM-41(62) at 813 K in air for 4 h

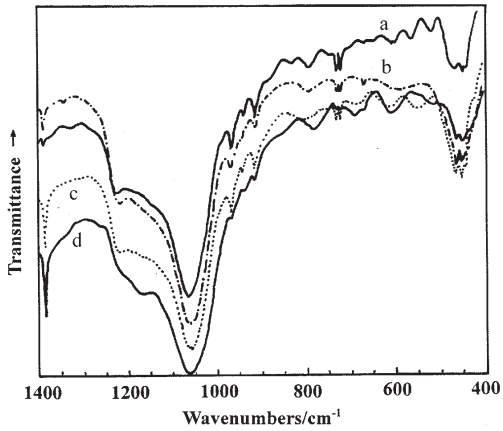

Fig. 10 Framework vibration FT-IR spectra for as-synthesized samples. a – SiMCM-41; b – FeSiMCM-41(124); c – FeSiMCM-41(62); d – FeSiMCM-41(32)

framework. Framework vibration FT-IR spectrum can also give information about the states of Fe(III) or La(III) species in zeolite molecular sieve samples. Figures 10–11 show the framework vibration FT-IR spectra for the as-synthesized FeSiMCM-41 and LaSiMCM-41 samples. It is evident that compared with the vibration bands for SiMCM-41, all the vibration bands of FeSiMCM-41 or LaSiMCM-41 shift to lower wavenumbers, indicating Fe(III) of La(III) may be incorporated into the channel wall [16–17], i.e., suggesting again the Fe(III) or La(III) species in these samples exist in a tetrahedrally coordinated environment.

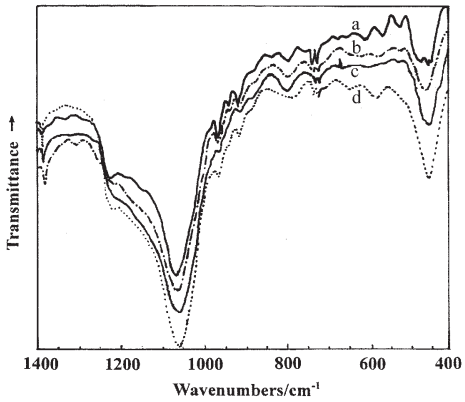

Fig. 11 Framework vibration FT-IR spectra for as-synthesized samples. a – SiMCM-41; b – LaSiMCM-41(147); c – LaSiMCM-41(83); d – LaSiMCM-41(48)

From the above discussion, we come to the conclusion that Fe(III) or La(III) species, at least partially, was incorporated into channel wall of as-synthesized Fe-containing or La-containing MCM-41 samples. However, comparing the lost contents corresponding to the steps associated with Fe(III) or La(III) species (Figs 6 and 7), we find that the lost contents increase with the increment of Fe(III) or La(III) contents for samples possessing relatively low Fe(III) or La(III) contents, but no linearity relationship between the lost content and the Fe(III) or La(III) contents in these as-synthesized samples is found. This shows us, the more the Fe(III) or La(III) content is, the more difficult the incorporation of these species into framework is. Especially, even though the Fe(III) content in FeSiMCM-41(32) is almost twice as much as that in FeSiMCM-41(62), the lost contents associated with Fe(III) species are nearly equal to each other. The situation can also be observed when investigating the framework vibration FT-IR spectra for as-synthesized samples. Although the bands for these samples generally shift to low wavenumbers with the increase of Fe(III) or La(III) content, the bands for FeSiMCM-41(32) do not demonstrate the same trend. Compared with those for FeSiMCM-41(62), the bands for FeSiMCM-41(32) shifts towards even high wavenumbers.

Compared with the behaviour of Fe(III) or La(III) species in Fe-containing or La-containing samples upon thermogravimetric analysis, the lost content associated with Al species in AlSiMCM-41 samples increases linearly with the Al contents in these samples (Fig. 5). It is supposed that the difference between the M–O bonds (*M*=Si, Al, Fe and La) is responsible for the different thermogravimetric behaviors of these as-synthesized samples. The length of Al–O bond (0.175 nm) is slightly longer than that of Si–O bond, making it easy for Al to insert into framework. However, Fe–O bond (0.197 nm) or La–O (0.254 nm) is much longer than Si–O bond, the incorporation of Fe(III) or La(III) into channel wall to replace Si–O bond will severely distort the tetrahedron MO_4 and is, therefore, more difficult than the incorporation of Al species. Thus, the content of Fe(III) or La(III) species in framework is very limited, no matter what the total content of these species in the as-synthesized samples is.

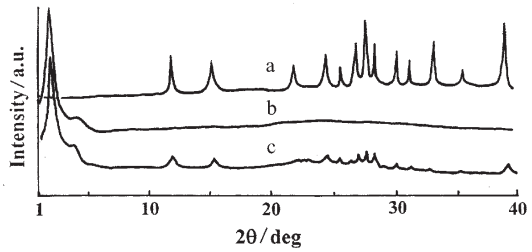

Fig. 12 XRD patterns for a – La_2O_3; b – calcined LaSiMCM-41(La_2O_3 6.1%) (813 K, 4 h); c – La_2O_3/SiMCM-41(La_2O_3 6.1%)

Because the Fe–O or La–O bond is longer, not only the incorporation of Fe(III) or La(III) into framework (channel wall) is limited, but also the Fe(III) or La(III) species is destabilized in framework. Upon calcination at 813 K in air to remove template, the Fe(III) species in FeSiMCM-41 samples gradually transformed from tetrahedrally coordinated state to octahedrally coordinated state [14], accompanied by the disappearance of ESR signal with g=4.3 (Fig. 8d) and the increase of Mössbauer IS value from 0.28 to 0.43 mm s^{-1} (Fig. 9b), meaning that Fe(III) species mostly migrated from framework to the outer surface of channel wall. La(III) species also transformed from framework state to non-framework state [14], but as shown in Fig. 12 no detectable La_2O_3 phase is found in calcined LaSiMCM-41(83) (Fig. 12b). In contrast to the appearance of La_2O_3 phase in the XRD pattern for the La(III) loaded SiMCM-41 sample prepared by mixing La_2O_3 and SiMCM-41 and possessing the similar La_2O_3 content as that in LaSiMCM-41(83) (Fig. 12c), it seems that after calcination the developed La(III) species highly dispersed on the surface of channel wall.

Conclusions

Results from thermogravimetric analysis, framework vibration Fourier transform infrared spectroscopic method, powder X-ray diffraction, electron spin resonance and Mössbauer spectroscopic techniques showed us that Fe(III) or La(III) species was in-

corporated into framework. Owing to the fact that Fe–O or La–O bond is longer than Si–O bond, Fe(III) or La(III) species was limited to insert into framework and transformed from tetrahedrally coordinated state to octahedrally coordinated state upon calcination to remove template.

* * *

This project was financially supported by the Natural Science Foundation of Hunan Province, China, the National Key Laboratory of Solid Microstructure of Nanjing University and the Science Foundation of Chinese Post-doctoral Programs.

References

1 C. T. Kresge, M. E. Leonowicz, W. J. Roth, J. C. Vartuli and J. S. Beck, Nature, 359 (1992) 710.
2 J. S. Beck, J. C. Vartuli, W. J. Roth, M. E. Leonowicz, C. T. Kresge, K. D. Schmitt, C. T- W. Chu, D. H. Olson, E. W. Sheppard, S. B. McCullen, J. B. Higgins and J. L. Schlenker, J. Am. Chem. Soc., 114 (1992) 10834.
3 A. Corma, V. Fornés , H. Carcia, M. A. Mirandin and M. J. Sabater, J. Am. Chem. Soc., 116 (1994) 9767.
4 R. Leon, D. Margolese, G. D. Stucky and P. M. Petroff, Phys. Rev. B, 52 (1995) R2285.
5 C. G. Wu and T. Bein, Science, 264 (1994) 1757.
6 C. G. Wu and T. Bein, Chem. Mater., 6 (1994) 1109.
7 C. G. Wu and T. Bein, Stud. Surf. Sci. Catal., 84 (1994) 2269.
8 P. L. Llewellyn, U. Decher, R. Stadler, F. Schüth and K. K. Unger, Stud. Surf. Sci. Catal., 84 (1994) 2013.
9 C. G. Wu and T. Bein, Science, 266 (1994) 1109.
10 D. H. Olson, G. D. Stucky and J. C. Vartuli, US Patent No. 5 364 797 (1994).
11 J. S. Beck, G. H. Kuehl, D. H. Olson, J. L. Schlenker, G. D. Stucky and J. C. Vartuli, US Patent No. 5 348 687 (1994).
12 T. Abe, Y. Tachibana, Takeshi and M. Iwamato, J. Chem. Commun., (1995) 1617.
13 P. Ratnasamy and R. Kumer, Catal. Today, 9 (1991) 329.
14 N.-Y. He, S.-L. Bao and Q.-H. Xu, Stud. Surf. Sci. Catal., 105 (1994) 85.
15 R. Schmidt, D. Akporiaye, M. Stocker and O. H. Ellestad, Stud. Surf. Sci. Catal., 84 (1994) 61.
16 T. Inui, O. Yamase, K. Fukuda, A. Itoh, J. Tarumoto, M. Morinaga, T. Hagiwara and T. Takegami, Proc. 8th Int. Conf. Catal., Berlin (West), Vol. III (1986) 569.
17 X. Wang and L. Chen, Acta Petrolei Sinica (Petroleum Processing Section), 10 (1994) 62.
18 R. Szostak, V. Nair and T. L. Thomas, J. Chem. Soc. Faraday Trans., I (1987) 487.
19 A. V. Kucherov and A. A. Slikin, Zeolites, 8 (1988) 110.